Deep brain stimulation effects on subthalamic nucleus oscillatory activity in Parkinson's Disease

Steffen Bürgers

(S1943626)

March 2015

Master Thesis MSc Behavioral and Cognitive Neurosciences c-track

Faculty of Mathematics and Natural Sciences

University of Groningen

Supervised by: Dr. M. Butz

Secondary evaluator: Dr. H. Van Rijn

Abstract

Objective: Deep brain stimulation (DBS) of basal ganglia nuclei such as the subthalamic nucleus (STN) is an effective treatment for symptoms of advanced Parkinson's Disease (PD). Yet, its mechanism of action remains poorly understood. In newly implanted patients it is possible to record local field potentials from the DBS electrode. However, the stimulation artifact has a much greater magnitude than physiological activity making inference problematic. Current evidence suggests that oscillatory dynamics in subcortical structures might be altered in a manner similar to treatment with medication, which includes a suppression of neuronal synchronization in the β-band, i.e. at 13-30 Hz.

Method: Here we investigate the oscillatory dynamics of local field potential recordings from the contralateral STN in response to unilateral DBS.

Results: During active DBS artifacts are evident even in the contralateral STN. Post-stimulation effects are not apparent, but the high variability both between and within patients and prominent broadband artifacts throughout several recordings make quantitative conclusions problematic.

Conclusions: Qualitatively β suppression seems to exist for some, but not all contralateral STN of PD patients. This study highlights the challenges, as well as the opportunities of post-operative local field potential recordings from the human subcortical structures.

Key words: Deep brain stimulation, Parkinson's Disease, subthalamic nucleus, neural oscillations, β-band

Acknowledgments

I want to thank my supervisor Markus Butz for his continued support, as well as the other members of the MEG DBS research group of HHU Düsseldorf for their help and suggestions, as well as fun and insightful discussions.

Table of Contents

Introduction

Parkinson's Disease

Parkinson's Disease (PD) is a debilitating neurodegenerative disorder that affects approximately 2% of the world population aged 65 and above (see Tan, 2013). It is classically characterized by a triad of motor symptoms, namely i) bradykinesia, denoting a slowing of movement often accompanied by akinesia, an inability to initiate movement or freezing, ii) rigidity and resistance to muscle movement, and iii) resting tremor. A further characteristic motor problem is postural instability (Xia & Mao, 2012). In addition, there are a number of secondary, less prevalent motor symptoms such as speech impairments and involuntary mirror movements on the contralateral side of an intentional action (Jancovic, 2008). Furthermore, a variety of non-motor symptoms tend to accompany the disease, including autonomic dysfunction, sleep disturbances, mood disorders, and decline of cognitive abilities (Sung & Nicholas, 2013).

The main pathophysiological feature of PD is a progressive loss of dopamine (DA) producing neurons in the *substantia nigra pars compacta* (SNpc), an important modulatory nucleus in the midbrain that is part of the *basal ganglia* (BG) motor system (Ohtsuka et al., 2013). Evidence suggests that PD has characteristics of a prion-disease, implicating α-synuclein as the prion protein (Olanow & Brundin, 2013). This is borne out by rare cases of genetic mutations in the α-synuclein gene, which lead to PD (Puschmann, 2013). Nevertheless, the vast majority of cases are still considered to be idiopathic and no cure or preventive measures are known.

Basal ganglia loops

Anatomically the basal ganglia (BG) are a collection of midbrain structures in the mammalian brain known as the *corpus striatum* (Str) and *globus pallidus* (GP). Functionally the BG additionally include the *substantia nigra pars reticulata* (SNpr), *substantia nigra pars*

compacta (SNpc), subthalamic nucleus (STN) and thalamus (Th). These structures form a number of structural and functional parallel loops that are crucial for voluntary movement initiation and inhibition of undesired motor plans, as well as non-motor processes like reward learning (reviewed in Nambu, 2008). Current models of the BG motor loops distinguish three pathways (Figure 1). The direct pathway consists of cortical areas projecting to the striatum, which in turn projects to the internal segment of the globus pallidus (GPi) and the SNpr (i.e. Cx-Str-GPi/SNpr-Th). GPi and SNpr send efferent projections to the thalamus, which sends information to the cortex, closing the loop. At rest GPi and SNpr tonically inhibit the thalamus, leading to a default state of inertia. When the cortex excites the striatum the thalamus is freed from that inhibition as the striatum now inhibits the GPi and SNpr. In contrast, the indirect pathway passes from the striatum through the external segment of the GP (GPe) and the STN (Cx-Str-GPe-STN-GPi/SNpr-Th) with a net effect of increased inhibition of thalamic activity. It is thought that the indirect pathway conveys a corollary discharge of conflicting motor plans (Nambu, 2008). At the level of the striatum both direct and indirect pathways receive modulatory afferents from the SNpc. For the most part, projections to excitatory D1 receptors are associated with the direct pathway and projections to the inhibitory D2 receptors are part of the indirect pathway (Lanciego, Luquin, & Obeso, 2012). Finally, the hyperdirect pathway bypasses the striatum and consists of an excitatory projection from the cortex to the STN and after that to the GPi and SNpr (i.e. Cx-STN-GPi/SNpr-Th). It is thought to be important for modulation of planned movements or inhibition of undesired motor plans (Nambu, 2008).

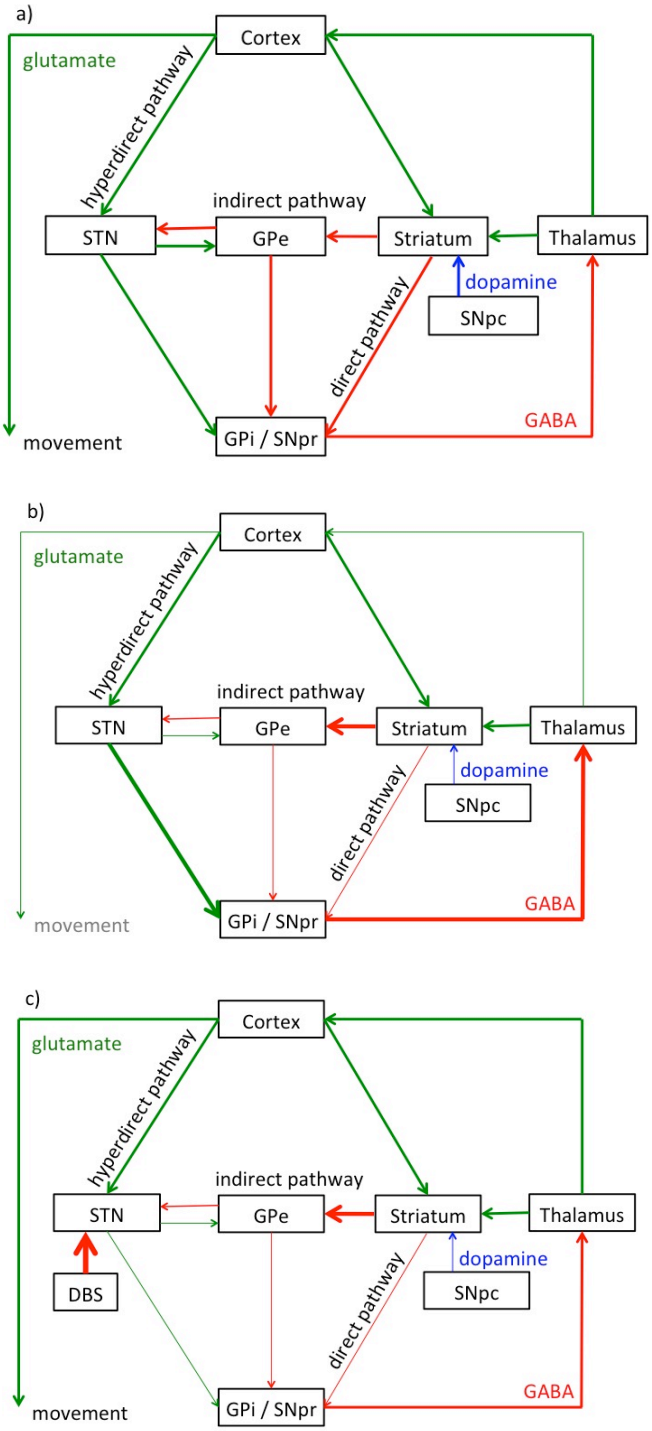

Figure 1. Basal ganglia motor loop in a) health, b) Parkinson's Disease, and c) Parkinson's Disease with deep brain stimulation of the STN. The schematics of b) and c) are a speculative illustration of the rate model (Albin et al., 1989). STN = subthalamic nucleus, GPe = external part of globus pallidus, SNpc = substantia nigra pars compacta, GPi = internal segment of globus pallidus, SNpr = substantia nigra pars reticulata. Modified from Nambu (2008).

Models of pathophysiological basal ganglia activity

The exact workings of the BG or changes that give rise to PD symptomatology are not fully understood. There are two main models pertaining to either changes in firing rate or changes in firing pattern of neuronal assemblies (Belluscio et al., 2014). The rate model is illustrated in Figure 1b. It poses that the lack of dopaminergic input to striatal medium spiny neurons (MSN) leads to reduced activity in the direct pathway and increased activity in the indirect pathway (Albin, Young, Penney, Roger & Young, 1989). According to the rate model a lesion or an inhibitory boost to the STN reduces the excitatory influence on the GPi and SNpr, therefore liberating the tonically inhibited thalamus (Figure 1c). This basic principle is supported by a number of findings, including direct modulation of either D1 or D2 receptors via optogenetics, which leads to the expected outcomes (Kravitz et al., 2010), as well as lesion and stimulation studies of the STN or GP in monkeys and corresponding surgical procedures in humans (see Kocabicak, Tan & Temel, 2012). However, even though it fits well with many experimental findings, the simple view of increased or decreased amplification of signals cannot account for all study results. While many studies did find expected firing rate differences, others failed to report an expected increase or decrease in firing rate and some actually found firing rate changes opposite the predicted direction (reviewed in Belluscio et al., 2014). Furthermore, the rate model does not take into account potential changes in the hyperdirect pathway and it neglects the functional significance of oscillatory changes in BG neural networks.

Instead of firing rate, the pattern model focuses on changes in oscillatory coupling within the BG, which is clearly different in the diseased state (e.g. Bergman et al., 1998). Animal models of PD using 6-hydroxydopamine (6-OHDA) in rats and 1-Methyl-4-phenyl-1,2,3,6-tetrahydropyridin (MPTP) in primates showed an increase in burst firing and oscillatory synchrony in BG structures compared to healthy controls (Mallet et al., 2008; Bergman et al., 1998). Furthermore, human PD patients consistently show a variety of

oscillatory patterns and couplings in subcortical, as well as cortical structures (Oswal, Brown & Litvak, 2013b). This includes strong synchrony in the β-frequency band in the STN (13-30 Hz), which is reduced by medication and proportional to clinical improvement (Hammond, Bergman & Brown, 2007; Eusebio et al., 2011). These changes in BG firing pattern in the diseased state might at least in part be explained by a defective gating of cortical rhythms at the striatal level (Belluscio et al., 2014). Support for this comes from the finding that a subset of up-states of striatal MSNs in rats synchronize with cortical activity. In healthy rats those sub-threshold fluctuations rarely cross action potential threshold due to D2-receptor afferents (Tseng, Kasanetz, Kargieman, Riquelme & Murer, 2001). However, in 6-OHDA-lesioned rats that inhibitory influence is attenuated leading to a rhythmic series of action potentials to efferent neurons in the GPe coupled to the cortical-striatal input and shifted in phase relative to that input (Belluscio et al., 2014). Inducing NMDA blockers in the striatum can abolish this coupling and normalize oscillations in the GP for low frequency bands (2.5 – 20Hz), but not for higher frequencies (Zold, Escanade, Pomata, Riquelme & Murer, 2012).

Therapeutic modulation of the basal ganglia

Since the late 1960s the focus of pharmaceutical therapy of PD symptoms has been to increase functional dopamine activity in the brain, first with the DA precursor amino acid L-3,4-dihydroxyphenylalanine (levodopa or l-dopa), and more recently with the introduction of DA agonists, monoamine oxidase B (MOA/B) inhibitors and catechol-O-methyl transferase (COMT) inhibitors (Maranis, Tsouli, & Konitsiotis, 2011). These treatments can be very effective, but have to be monitored carefully to minimize side effects. Furthermore, artificially increasing dopamine levels or activity in the brain by introducing chemicals via the blood stream is inevitably unspecific and cannot substitute for the natural dopamine distribution that depends on an intricate network of synapses and multiple receptor types (Chinta & Andersen, 2005; Beaulieu & Gainetdinov, 2011). Common long-term side effects

include dyskinesia, impulse control problems and psychosis (Maranis et al., 2011; Sung & Nicholas, 2013). Consequently, as the disease progresses effective pharmaceutical treatment of PD symptoms without the emergence of unpleasant side effects becomes less and less likely.

An alternative to medication is the implantation of an electrical pacemaker into structures of the BG motor loop like the STN (Hung, Tsai, Lin, Jiang & Chen, 2013). Motor symptoms as assessed by Unified Parkinson's Disease Rating Scale (UPDRS) scores are improved approximately by a factor of 0.5, similar to the reduction in l-dopa dose (Eusebio, Cagnan & Brown, 2012). Importantly, DBS side effects are reversible and stimulation parameters can be fine tuned for the individual patient, maximizing treatment benefits. In spite of the therapeutic success of DBS the actual mechanism by which it leads to symptom reduction remains unclear (McIntyre & Hahn, 2010). For example, a commonly used stimulation frequency is 130 Hz, but frequencies in the γ-band (50-100 Hz) or even higher stimulation frequencies show beneficial effects as well (Tsang et al., 2012; Garcia, D'Alessandro, Bioulac & Hammond, 2005), whereas low frequency stimulation in the α- or β-band (7 – 30 Hz) were either ineffective or have been associated with a worsening of symptoms (Garcia et al., 2005). Even though individual stimulation frequencies and amplitudes can be optimized, this procedure can take considerable time and often has to be adjusted to remain effective as the disease progresses. A recent area of research are closed-loop DBS systems, which send stimulation pulses informed by simultaneous local field potential (LFP) recordings and dynamically try to suppress local β-activity, so far with promising results in monkeys (see Beuter, Lefaucheur & Modolo, 2014).

Oscillatory activity and synchronized neural networks

From a scientific perspective, a great advantage of deep brain stimulation implants is that apart from stimulation of neurons the local electric field of the brain region can be

recorded. This local activity can then be related to electric or magnetic activity measured near the patient's scalp. The organization of the mammalian brain into functionally distinct regions and the small world property in which the cortical network is organized supports the integration of information from ongoing activity via transient synchronous oscillations (Buzsáki & Draguhn, 2004). Consequently, by probing oscillatory activity it is possible to at least in part discern the neural communication patterns that underlie behavior. With respect to Parkinson's Disease a variety of findings have emerged that show a change in oscillatory dynamics after medication, as well as DBS treatment at rest or during movement (see Oswal, Brown & Litvak, 2013b; Brittain & Brown, 2014). Those are going to be discussed in more detail below. For an overview see Figure 2.

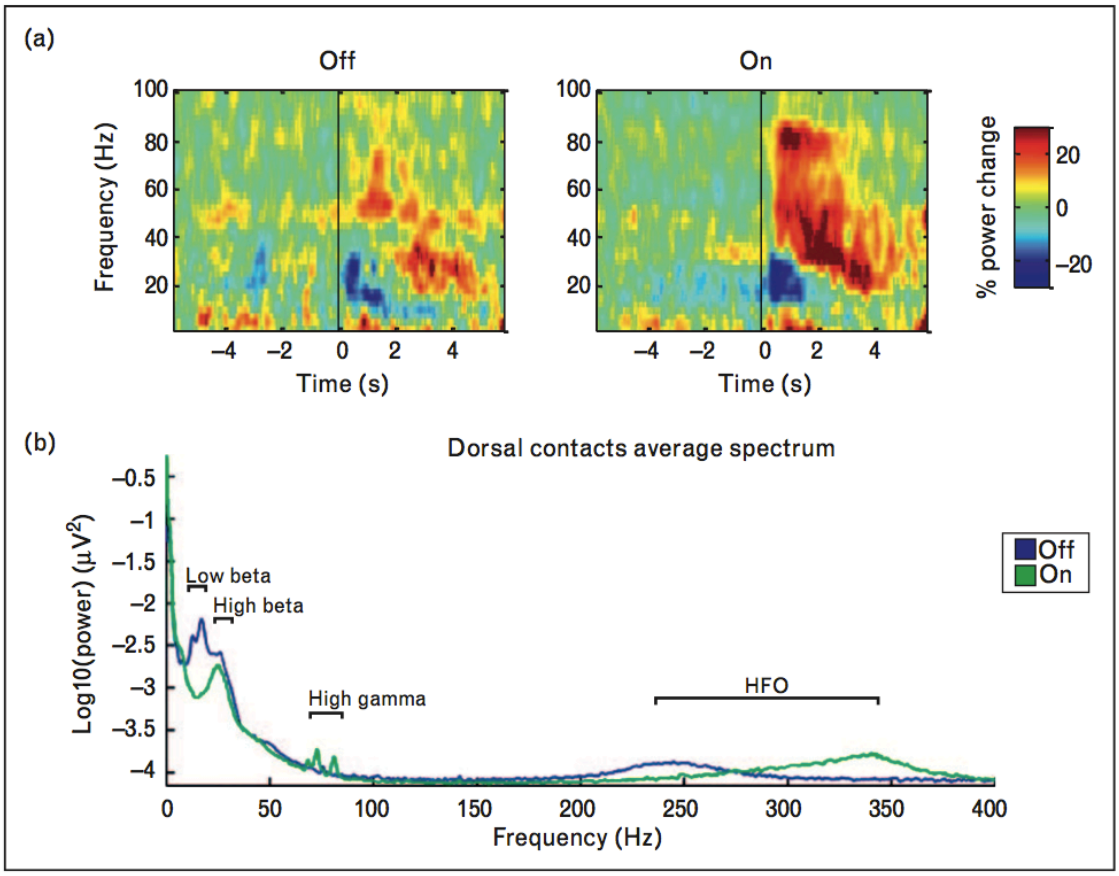

Figure 2. (a) Time-frequency representations of STN power of PD patients in ON and OFF states of l-dopa medication. The time axis is anchored at onset of a movement instruction. Retrieved from Oswal et al. (2013b). (b) Power spectral density differences ON and OFF levodopa measured at STN of PD patients. Retrieved from López-Azcárate et al. (2010).

β-band (13-30 Hz). At the cortical level, a common finding with regard to β-power is that it is suppressed prior to and throughout voluntary movement, followed by a rebound of increased synchrony. Moreover, stimulating the cortex at β-frequencies during movement reduces motor activity (reviewed in Brittain et al., 2014). A similar movement related suppression of β-power is observed in the LFP recordings of PD patients at the STN level (Joundi et al., 2012b). In addition, power in the β-frequency band in basal ganglia structures including STN (Kühn et al., 2009) and GPi (Silberstein et al., 2003) is elevated in the OFF medication state compared to ON medication when patients are at rest. Furthermore, the degree of l-dopa suppression of β-power correlates with improvement of bradykinesia and rigidity, but not tremor scores (Kühn et al., 2009), and variations in β-power are associated with ongoing fluctuations in symptom severity (Little, Pogosyan, Kühn, & Brown, 2012). It has also been found that subcortical β-activity is coupled with and driven by cortical β-band oscillations (Hirschmann et al., 2011; Litvak et al., 2011). However, cortical oscillations are in the upper spectrum of the β-band, whereas subcortical rhythms are more prominent in the lower part of the spectrum, which is also much more responsive to l-dopa medication (López-Azcárate et al., 2010). With respect to DBS, it has been postulated that stimulating at the electrode site with the highest β-power is more efficient and necessitates lower stimulation amplitude compared to other electrode sites (Yoshida et al., 2010). Furthermore, it has been shown that intra-operative recordings from adjacent bipolar DBS electrode contacts detect a marked increase in β-synchrony when entering the dorsal STN as indicated by stun effects and post-operative stereotactic MRI (Chen et al., 2006).

These findings point to a close connection between elevated β-synchronization and motor problems. Nevertheless, establishing a direct relationship between β-oscillations and motor impairment is not completely straightforward. The degree of synchronization in the STN OFF medication has been found to be associated with motor impairments in some studies (e.g. Özkurt et al., 2011), but not others (e.g. Kühn et al., 2009). Furthermore,

stimulation of the STN at low frequencies in and around the β-band decreases finger tapping speed (Eusebio et al., 2008) and maximum grip force (Chen et al., 2011), but only slightly. It is not clear whether these changes are small due to ceiling effects of possible β-synchronization, the discrete and static nature of the stimulation pulses, or the distributed characteristics of the oscillatory network, which is not only comprised of the nucleus at the stimulation site (see Eusebio et al., 2009). Nevertheless, even if the relationship between β-oscillations and motor symptoms is not completely understood, it is undoubtedly a very important frequency band with regard to movement and motor symptoms in PD and can be used constructively in DBS treatment approaches (Yoshida et al., 2010; Beuter, Lefaucheur & Modolo, 2014).

α-band (8 – 12 Hz). In addition to the cortico-subcortical β-network described above, a parallel, more diffuse STN-temporoparietal network in the α-frequency band has been identified via LFP and simultaneous magnetoencephalography (MEG) recordings of PD patients (Hirschmann et al., 2011; Litvak et al., 2011). This α-network shows a reduction in oscillatory coupling during voluntary action, in particular in the ON state (Oswal, Brown & Litvak, 2013a) and might be related to attentional processes (see Oswal et al., 2013b). Apart from that there is also evidence for subcortical α-power to be associated with tremor severity as opposed to bradykinesia and rigidity in case of β-band power (see Beuter et al., 2014).

γ-band (30 – 100 Hz). Another spectral band associated with movement has been identified in the finely tuned γ-band (FTG) between 60 and 90 Hz. Oscillatory power in this frequency band at subcortical sites is elevated during voluntary movement and has been interpreted as vigor or effort of an action, but a direct causal role is contentious (Oswal et al., 2013b). Support for this hypothesis comes from the finding that cortical stimulation of healthy participants at FTG frequencies augments grip force (Joundi, Jenkinson, Brittain, Aziz & Brown, 2012a). Furthermore, l-dopa medication has been found to increase FTG power in the STN, but these effects are only apparent in a subset of STN LFPs recorded by

macroelectrodes (see Jenkinson, Kühn & Brown, 2013).

HFO (> 100 Hz). High frequency oscillations (HFOs) above 200 Hz are associated with voluntary movement and more pronounced in ON versus OFF states. Furthermore, the ratio of fast HFOs (300-400 Hz) to slow HFOs (200-300 Hz) reliably distinguishes STN recordings from ON and OFF state (Özkurt et al., 2011). For an illustration of HFO reactivity to medication see Figure 2. In addition, there is pronounced phase amplitude coupling (PAC) between β and HFOs in the ON state, which is markedly reduced in the OFF state (López-Azcárate et al., 2010; Özkurt et al., 2011). Interestingly, there is also β-phase locked spiking, which similar to β-HFO-PAC is most prominent in the dorsal STN compartment. Despite this, there is no obvious relationship between the two measures raising the interesting question what mechanism if not rhythmic spiking underlies those β-phase coupled HFOs (Yang, Vanegas, Lungu & Zaghloul, 2014). Moreover, Özkurt and colleagues (2011) found that fast HFO to slow HFO ratio was associated with UPDRS akinesia and rigidity scores, as was β-power. However, there was no significant correlation between the two and HFO power ratio explained more UPDRS score variance than did β-power (ratio of 76 to 24). These findings implicate HFOs as functionally relevant in PD and movement and partially associated with β-band-oscillations. In fact an interesting possibility is that the adverse effect of increased β-power in the Parkinsonian state might be indirect and emerge from its modulation of HFOs (see Storzer, Bürgers & Hirschmann, 2015).

Deep brain stimulation and oscillatory dynamics

Therapeutic effects of DBS remain for some patients after ceasing stimulation for an interval of seconds to tens of seconds, with longer after effects for longer stimulation periods (Kühn et al., 2008). Those positive after-effects were found to decrease gradually and correlate with the degree of β-suppression relative to pre-stimulation baseline levels, which also slowly normalized after ceasing stimulation (Kühn et al., 2008). Lasting post DBS

β-suppression when patients are at rest has also been found during intraoperative recordings of two patients (Wingeier et al., 2006), as well as in a larger patient sample (Bronte-Stewart et al., 2009). On the other hand, others failed to find such after-effects (Foffani et al., 2006). Furthermore, Rossi and colleagues (2008) actually managed to record LFP activity during DBS and found no β-suppression, but an increase in low frequency power (< 7 Hz), which slowly returned to baseline after stimulation was turned off. Such post-stimulation slow wave power increases were also found by others (Priori et al., 2006). One possible explanation of these seemingly conflicting findings with respect to β-modulation might be differences in patient selection and choices of time periods of interest. Rossi and colleagues (2008) allowed for patients to be medicated, which is known to suppress β-power independently of stimulation (e.g. Kühn et al., 2008). Whereas Foffani et al. (2006) tested for a post-stimulation effect in a 60 second window average, which might not capture more short lived effects as for example observed in Bronte-Stewart et al. (2009). Indeed, a later study recording LFPs during DBS specifically investigated the interaction between levodopa and DBS with respect to β-oscillations (Giannicola et al., 2010). The authors found that both DBS and l-dopa medication suppress β-activity, and that the effect of l-dopa is more powerful, leaving no additive effect of DBS in a medication ON state.

Study objectives

An important goal in PD research is to meaningfully interpret neurophysiological recordings at the LFP and scalp level during DBS, which is hampered by the strong electrical activity in stimulation wires and electrodes. Most studies have up to now investigated DBS influences by considering stimulation after effects at the STN that had been stimulated (see Eusebio et al., 2012). The current study was designed to investigate LFP activity from the STN contralateral to the stimulation site. Consequently, we can explore whether or not the stimulation artifact has a detrimental effect even on the contralateral hemisphere's LFP

signals, and assuming that this is not the case, investigate contralateral physiological activity. In addition, we are going to explore post-stimulation effects on both ipsilateral and contralateral STN. Even though there is no direct anatomical bridge between both STN, functionally the two nuclei do show connectivity, for example in the form of α-band (8-12 Hz) phase locking in relation to voluntary unilateral finger tapping (Darvas & Hebb, 2014). Moreover, unilateral DBS is effective for alleviating both ipsilateral and contralateral motor symptoms (Shemisa et al., 2011). Therefore it seems plausible that there might be bilateral reactions to unilateral DBS in the form of oscillatory changes. Another goal of this study is to investigate the effect of different DBS frequencies, namely either 130 Hz or 340 Hz.

First, we hypothesize that synchrony in the β-band (13-30 Hz) is reduced during DBS on the contralateral side, akin to the effect of medication and DBS on the ipsilateral side. Furthermore, individual power peaks in the β-band are expected to show continued suppression after DBS has ceased and slowly return to baseline levels for both ipsilateral and contralateral STN.

Secondly, we also cautiously expect increased slow wave power below 7 Hz after stimulation relative to baseline, which slowly normalizes post DBS.

Thirdly, HFOs are predicted to show a modulation around the 250 Hz and 350 Hz bands. Specifically, contralateral STN during stimulation and both STN after stimulation are expected to show a shift in power ratio between these two bands in favor of the 350 Hz peak as a consequence of stimulation. Again these effects are expected to taper off post-DBS.

Finally, with respect to stimulation frequency, we expect that both 130 Hz and 340 Hz will lead to the aforementioned outcomes albeit possibly to different degrees, with highest discrepancies expected in HFOs around 350 Hz due to the proximity to the 340 Hz DBS frequency.

Method

Disclaimer

The student did not partake in the data acquisition process for the data under study. This was not possible due to the nature of this patient research which needs to collect data over longer time spans, i.e. several months or even years and is only projectable in a limited way. However, the student joined running MEG-DBS recordings of the current projects and thus, could experience the nature of these experiments and the research techniques at hand. The following information is based on experimental protocols and consultation with staff who carried out the recordings.

Patients

In total 17 patients with PD participated in the study (3 women, M_{age} = 62.59 years, SD_{age} = 9.66 years, age range = 44–74 years). All patients were selected for surgical implantation of DBS electrodes in order to alleviate disease symptoms and medication side effects. Spectral analyses were carried out on a subset of patients depending on availability and cleanliness of the data. Five patients were excluded from all spectral analyses. Two data sets were excluded due to insufficient noise-free baseline data and two showed very strong artifactual activity in the post-stimulation period, leaving insufficient clean data. Another data set was excluded due to high impedance (> 20000 Ω) in all bipolar contacts.

Patients signed an informed consent declaration for study participation, which was approved by the local ethics board and is in accordance with the Declaration of Helsinki. An overview of patient characteristics can be seen in Table 1. Experienced staff of the University Hospital Düsseldorf carried out the measurements and data acquisition.

Table 1

Detailed patient information

Patient	Sex	Age (years)	UPDRS pre OP	UPDRS post OP	Medication pre OP	Medication post OP
1	M	49	33	22	OFF	OFF
2	M	66	41	48	m.d.	OFF
3	M	64	38	26	m.d.	OFF
4	M	71	43	21	OFF	OFF
5	M	44	21	13	OFF	OFF
6	M	70	15	30	ON	OFF
7	F	44	52	65	OFF	OFF
9	M	65	31	m.d.	OFF	OFF
10	M	57	m.d.	31	m.d.	OFF
11	F	66	m.d.	30	ON	OFF
12	M	52	40	36	OFF	OFF
13	M	68	24	27	OFF	OFF
14	M	70	44	37	transition to ON	OFF
15	M	74	22	49	OFF	OFF
16	M	71	22	33	OFF	OFF
17	F	67	43	33	OFF	OFF
18	M	68	17	15	OFF	OFF
Mean		62.59	32.4	32.25		
Sd		9.66	11.54	13.21		

Note. UPDRS scores are summed over bradykinesia and rigidity scales. Abbreviation "m.d." denotes missing data, "Sd" means standard deviation.

Surgery

Stimulation electrodes were implanted at the Department of Functional Neurosurgery and Stereotaxy of the University Hospital Düsseldorf, Germany. The evening before surgery oral medication was withdrawn and subcutaneous apomorphine was administered instead. The head was fixated with a Riechert-Mundinger Frame. Patients were anaesthetized locally in order to be able to give conscious feedback during intracranial microelectrode stimulation and guide electrode placement. The desired region of the STN was located 12 mm lateral from midline, 3 mm behind the mid-commissural point and 4 mm below the AC-PC line.

Those coordinates were modified on an individual basis depending on stereotaxic preoperative T2 weighted MRI images, as well as microelectrode recordings and stimulation during the operation. Finally, correct placement was verified via computer tomography (CT) post-surgery.

Recordings

Recordings were acquired from MEG gradio- and magnetometers over the whole scalp, from non-stimulating electrodes in/near the STN, from horizontal EOG sites, and from EMG electrodes on the *musculus extensor digitorum communis* and *musculus flexor digitorum superficialis* on both arms.

For DBS one of two electrode systems was used depending on the patient. Thirteen patients received the DBS Lead Model 3389 by Medtronic Inc. (Minneapolis, MN, USA), and four patients were implanted with electrodes by St. Jude Medical (St. Jude Medical Inc., St. Paul, MN, USA). Both, Medtronic and St. Jude leads contain four stimulation/measurement contacts (see Figure 2). DBS lead electrode signals were referenced to averaged mastoid signals online. MEG recordings were made with an Elekta Neuromag 306 whole head system (Elekta Oy, Helsinki, Finland). This device contains 102 sensor triplets each consisting of two gradiometers and one magnetometer resulting in a total of 306 channels. EMG was recorded with non-magnetic ANBU Neuroline 720 electrodes (Ambu, Ballerup, Denmark). Bipolar EMG channels were obtained from muscle belly-tendon pairs. For horizontal and vertical electrooculogram four 5mm Ag/AgCl electrodes were used yielding two bipolar channels. By default the 13-pair was chosen for stimulation, which was changed only, if stimulation was not possible at this site for example due to excessively high impedance.

Data was acquired at a sampling rate of 2 kHz. An online band-pass filter was applied to MEG signals (0.03 – 660 Hz), as well as to EMG, EOG and LFP signals (0.1 – 660 Hz).

Procedure

Participants were contacted as soon as they arrived at the hospital and pre-operational recordings were made at a convenient time prior to the date of surgery. UPDRS scores were measured before the recording of physiological activity and usually happened on the same day as the other recordings, with one exception where UPDRS outcomes were assessed one day earlier. Post-operational measurements took place a day or two after surgery, which was required, as the second surgery for implantation of the stimulation device was scheduled two days after the first. Most pre-operational recordings (n = 11) and all post-operational recordings were done OFF medication (see Table 1). For post-operational recordings the apomorphine pump was turned off ≥ 90 min. prior to the beginning of the recording session.

Patients were instructed to sit relaxed with eyes open during measurements, while their arms were rested on a small table that could be attached to the MEG system chair. First, a three-minute period of resting activity without stimulation was recorded, followed by four three-minute stimulation intervals interleaved with one-minute intervals of no stimulation. In the end, another three minutes of resting, non-stimulated activity was recorded. This procedure was planned to be repeated for all stimulation frequencies (5 Hz, 20 Hz, 130 Hz, 260 Hz, and 340 Hz; see Figure 3). Focus was put on stimulation frequencies 130 Hz (n = 16) and 340 Hz (n = 13), and many patients were unable to complete recordings for more than those two frequency bands.

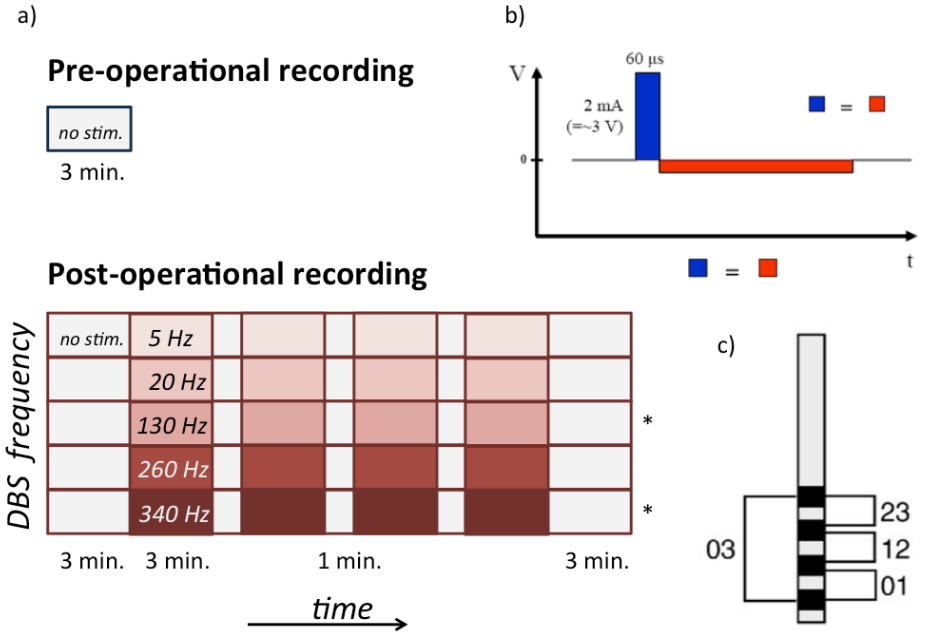

Figure 3. (a) Outline of the experimental paradigm. Asterisks denote the DBS frequencies analyzed in this thesis. (b) Stimulation pulse characteristics. (c) Schema of the DBS electrode contacts. The labels denote bipolar rereferencing where numbers descent from dorsal to ventral.

Preprocessing

Data preprocessing and analyses were carried out with the analysis software provided by Elekta Neuromag (Elekta Oy, Helsinki, Finland) and the Fieldtrip toolbox (Oostenveld, Fries, Maris, & Schoffelen, 2011) for Matlab (The Mathworks Inc., 2014). Data was downsampled to 1024 Hz to speed up subsequent analyses and save disk space. Raw EMG data were inspected visually for all conditions in order to classify periods of tremor and movement artifacts. Similarly, data from LFP channels were surveyed to denote post-stimulation signal saturation and other artifacts.

Artifact rejection

All analyses were carried out on cleaned data, i.e. without time periods classified as tremor, muscle, saturation, or jump artifacts. Periodograms for all adjacent bipolar channel montages were plotted and visually inspected to ensure plausibility and cleanliness of the data before choosing a contact pair per STN (see Figure S1). The time-domain data of the final channel selection was inspected visually in order to exclude remaining jump or saturation artifacts. Ipsilateral channels frequently showed strong artifactual activity even in stimulation OFF periods. Therefore artifacts were rejected solely based on the contralateral channels.

Channel selection

Adjacent channel pairs on the contralateral side of stimulation were rereferenced with one another to narrow down the likely origin of the signal to a more confined region. As stimulation electrodes were not connected for recording the ipsilateral side relative to stimulation contained only one bipolar contact. That contact was either 02 or 13 (see Figure 3). It has previously been shown that β-power measured from bipolar DBS electrode contacts can be a reliable marker for STN localization, both during surgery (Chen et al., 2006), and when compared to post-operative MRI scans (Chen et al., 2006; Kühn, Kupsch, Schneider & Brown, 2006; Kühn et al., 2008). Accordingly, the bipolar signal with the highest β-power (13 – 30 Hz) in the rest period prior to any DBS was chosen as a likely substrate of STN activity.

Spectral analyses

Power spectral density (PSD) estimates were obtained using Welch's method in order to reduce variance (Welch et al., 1967). Data were segmented into 1 s pieces with half a second overlap. Each segment was convolved with a Hanning taper in order to reduce spectral leakage. The modulus of the discrete Fourier transform was averaged over all windows to

obtain the PSD estimate. Spectrograms were created with a 1 second time window moving in steps of 0.1 s yielding a frequency resolution of 1 Hz.

Spectral estimates of high frequency oscillations (i.e. above 160 Hz) were obtained with a multitaper approach using discrete prolate spheroidal (Slepian) sequences (dpss; Thomson, 1982). Instead of using multiple samples of the signal of interest for PSD estimation this method applies several orthogonal tapers to each time window and averages over them. Spectral smoothing was set to increase with frequency (range: 4.8-11.7 Hz), whereas time windows became narrower (range: 0.938-0.385 s). This is sensible as the neurophysiological HFOs of interest span a broader frequency range than slower oscillatory activity, for example in the α- or β-band. Parameters were chosen so that eight Slepian sequences were applied as tapers.

Peak frequencies in the β-band were determined automatically by finding the highest local peak power in the frequency band 13 – 30 Hz. Peak power was defined as average power in a 10 Hz range around the local peaks. Automatic peak detection was verified by visual inspection of periodograms.

Table 2

DBS settings

Patient	Lead model	STN	Stimulation channels	DBS current (mA)	Impedance
1	Medtronic	left / right	left 1-3	2 mA	2005 Ω
2	Medtronic	left / right	right 1-3	2 mA	1900 Ω
3	Medtronic	left / right	right 1-3	1 mA	1831 Ω
4	Medtronic	left / right	right 1-3	2 mA	1778 Ω
5	Medtronic	left / right	left 1-3	2 mA	1132 Ω
6	Medtronic	left / right	right 1-3	2 mA	1610 Ω
7	Medtronic	left / right	right 1-3	2 mA	1996 Ω
9	St. Jude	left	left 1-3	2 mA	1075 Ω
10	St. Jude	left / right	right 0-2	1.5 mA/130 Hz 1 mA/340 Hz	1096 Ω
11	St. Jude	left / right	right 1-3	2 mA	1060 Ω

12	St. Jude	left / right	right 1-3	2 mA	582 Ω
13	Medtronic	left / right	left 1-3	2 mA	2162 Ω
14	Medtronic	left / right	left 1-3	1.5 mA	1887 Ω
15	Medtronic	left / right	left 0-2	2 mA	1471 Ω
16	Medtronic	left / right	left 1-3	2 mA/130 Hz 1 mA/340 Hz	1654 Ω
17	Medtronic	left / right	left 1-3	2 mA	1448 Ω
18	Medtronic	left / right	right 1-3	1 mA	1760 Ω

Note. The abbreviation "m.d." denotes missing data.

Data analysis

Statistical analyses were carried out with the open source software R (R core team, 2012), including the ggplot2 package for graphical depiction (Wickham, 2009), and the Fieldtrip toolbox of Matlab (Oostenveld et al., 2011). Repeated measures ANOVA was carried out with the ez package (Lawrence, 2012). Mixed effects models were fitted with the lme4 package (Bates, Maechler & Bolker, 2011). Confidence intervals for within patient analyses were computed according to Cousineau (2005) and Morey (2008) with the code provided by Baguley (2012). Evolution of peak power in the β-band (13-30 Hz) post-stimulation was analyzed with pairwise t-tests. The data was log-transformed in order to fulfill the normality of residuals requirement as indicated by quantile-quantile-plots and Shapiro-Wilk tests.

Exploratory analyses of spectral power that is not based on individual frequency bands per patient were performed with a non-parametric cluster permutation test in order to avoid multiple comparison problems (Maris & Oostenveld, 2007). The permutation test is based on the hypothesis that the joint probability distribution of the two conditions is exchangeable, i.e. $f(D_{s1}, D_{s2}) = f(D_{s2}, D_{s1})$, where D is the population distribution of the time-frequency matrix of the dependent variable for a given patient s averaged over conditions 1 and 2 respectively. Based on this assumption any chosen test statistic will be equal between different permutations of (D_{s1}, D_{s2}) and a Monte Carlo simulation gives a p-value to test this

assumption. In this thesis a paired t-test was calculated for each time-frequency sample. T-values were assigned to clusters according to their proximity on the time-frequency axes and on the significance of the t-statistic at the level $\alpha = 0.05$. This way we take into account that any adjacent time-frequency samples are likely to be dependent on the same underlying event. The value of a cluster is given by the sum of its t-values. Subsequently the conditions for each participant are randomly reassigned (i.e. condition A becomes condition B and vice versa for a random number of participants). From this the t-matrix is again calculated and the summed t-values for each cluster are found. The largest summed t-value is the test-statistic. This process starting from the random reassignment of conditions is repeated a large number of times (n=1000) in order to obtain an accurate approximation of the Null-distribution (i.e. assuming that (D_{s1}, D_{s2}) is exchangeable). Finally, significant clusters in the original data are identified as cluster summed t-statistics falling outside of the Null-distribution given a specified α-value (cluster-$\alpha = 0.05$). The comparison of multiple clusters to the Null-distribution is unproblematic in terms of false discovery rate, because taking only the maximum cluster sum t-value per permutation for creating the Null-distribution holds the second (and third, fourth, etc.) strongest cluster to the same rigorous standard as the first cluster.

Results

The baseline period consisted of a three-minute period of simple rest recordings before any DBS (*m* = 97.79 s, *sd* = 37.85 s, *range*: 44 – 165.89 s, *n* = 12). Only few patients showed a distinct β-peak on the contralateral side during the baseline period (e.g. p10; see Figure 4). During DBS the stimulation artifact could clearly be observed in both hemispheres (see Figure S2 for an example). Therefore, no analyses were performed on stimulation ON data. The post-stimulation period lasted for 60 s. After artifact rejection most patients retained a continuous trial-averaged spectrogram (Figure S3 & S4). Grand average time frequency

evolution of the post-stimulation period is shown in Figure 5. The progression of peak-power in the β-band after ceasing DBS compared to the baseline period was tested by dividing the post-stimulation period into six 10-second bins (Figure 6). An overview of number of data points for each time bin can be seen in Table 3.

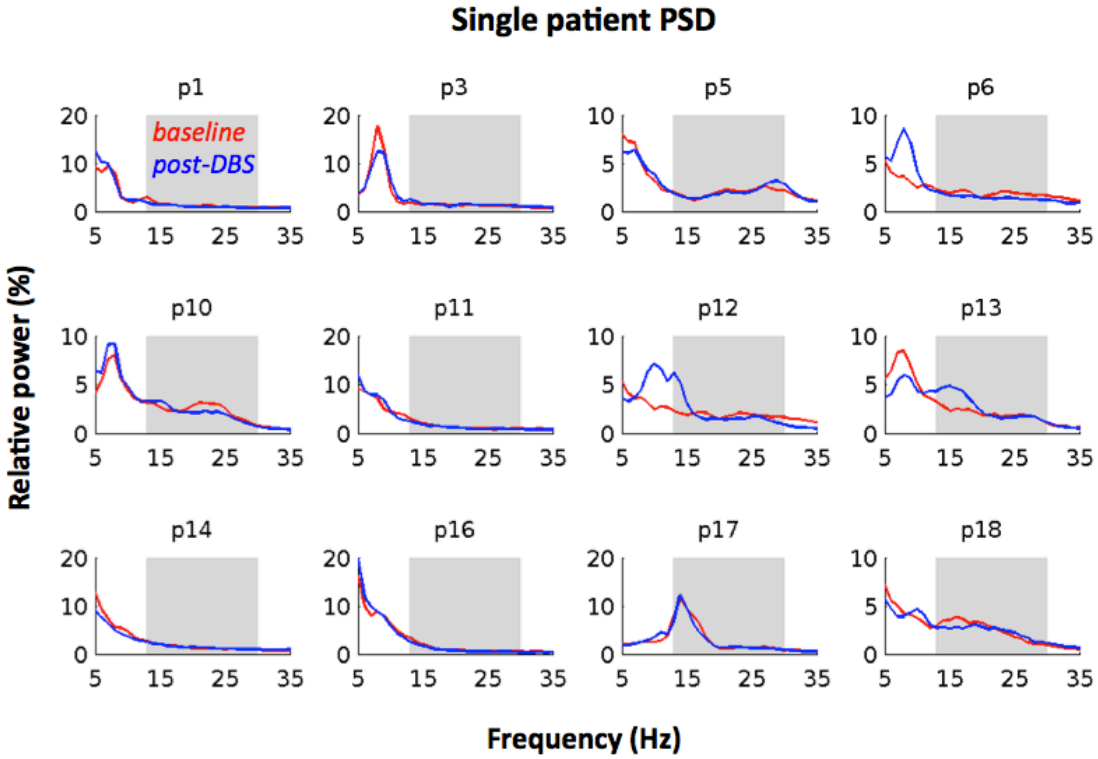

Figure 4. Periodograms of baseline PSD (red) contrasted with post-DBS PSD (blue) of the channel selection contralateral to the DBS hemisphere. Y-axes denote the percentage of total power between 5 and 95 Hz to facilitate visual comparison. Headings denote patient indices. Gray background denotes the β-band (13-30 Hz). Note the absence of distinct β-peaks in many baseline channels.

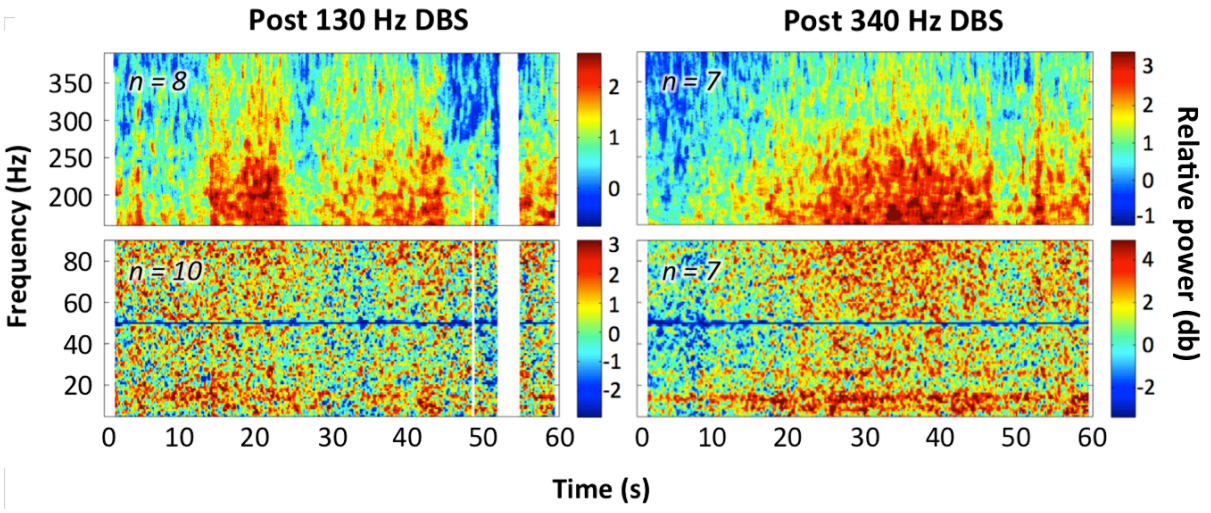

Figure 5. Post stimulation grand average spectrograms in the frequency ranges 1-90 Hz and 160-390 Hz showing power on a decibel scale relative to the baseline period. White areas denote missing data due to artifact rejection in at least one of the patient trial-averaged spectrograms.

Table 3

Available data post-DBS

Time bin (s)	Number of trials			Time per trial (s)			N
	Avg 130/340	Sd 130/340	Range	Avg 130/340	Sd 130/340	Range 130/340	130/340
0 – 10	2.3 / 2.4	1.1 / 1.1	1 - 4	6.7 / 7.4	2.5 / 2.1	1.1 - 9.6/ 2.3 - 9.5	42 / 32
10 – 20	2.4 / 2.4	1.1 / 1.1	1 - 4	8.1 / 8.9	2.8 / 2.2	0.6 - 10/ 2.9 - 10	43 / 32
20 – 30	2.3 / 2.4	1.1 / 1.1	1 - 4	9.2 / 9.4	1.3 / 1.3	5.6 - 10/ 4.7 - 10	42 / 33
30 – 40	2.3 / 2.3	1.1 / 1.1	1 - 4	8.7 / 9.0	2.3 / 1.8	2.2 - 10/ 4.1 -10	41 / 32
40 – 50	2.3 / 2.3	1.1 / 1.1	1 - 4	8.3 / 8.7	2.8 / 2.4	1 - 10/ 0.9 - 10	40 / 32
50 – 60	2.3 / 2.3	1.1 / 1.1	1 - 4	8.6 / 8.3	2.1 / 2.3	1.2 - 10/ 2.2 - 10	40 / 32

Note. The amount of missing data is relatively uniform.

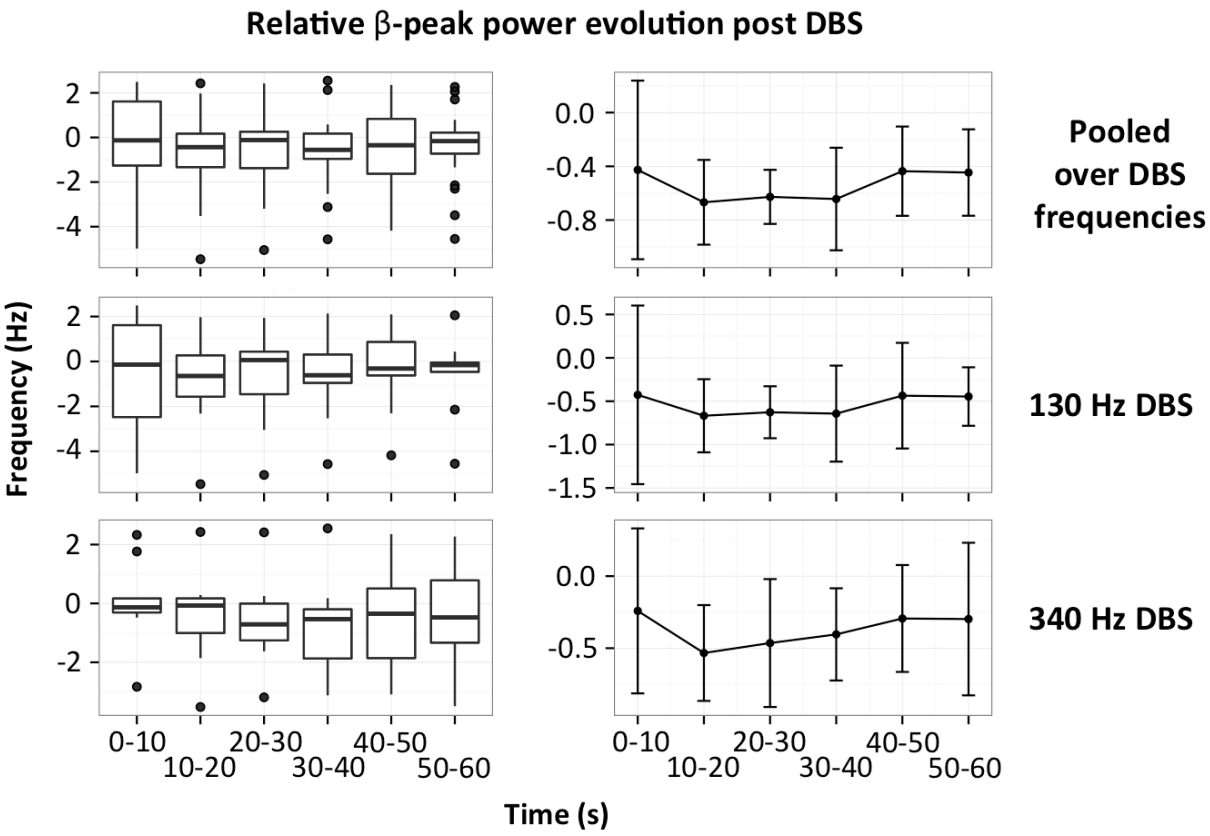

Figure 6. Percentage changes in log-transformed β-peak PSD post DBS relative to baseline. Boxplot rectangles denote the region between the first and third quartile. Lines connect to the last data point within 1.5 times the interquartile range from the median. Circles denote outliers. Error bars are 95% Cousineau Morey confidence intervals.

β -band

There was no significant percentage change in log-transformed peak-power comparing post-stimulation to baseline levels for neither 130 Hz, nor 340 Hz conditions as indicated by a two-way repeated measures ANOVA. Specifically, for stimulation frequency, $F(1, 8) = 0.31$, $p = 0.59$, $\eta^2_G = 0.00$, for time bin, $F(5, 40) = 1.16$, $p = 0.66$, $\eta^2_G = 0.00$, and for the interaction between stimulation frequency and time bin, $F(5, 40) = 4.06$, $p = 0.26$, $\eta^2_G = 0.02$. The p-value for the time factor is corrected for violations of sphericity with the Greenhouse Geisser method. Effect sizes denote generalized eta squared (Olejnik & Algina, 2003). In order to augment statistical power a linear mixed effects analysis was tried, enabling the

inclusion of three additional data sets that had to be excluded from the ANOVA due to missing data in the 340 Hz stimulation condition. However, comparing models with increasing complexity starting with only patients as random factor, and subsequently including time bin and stimulation condition as categorical fixed effects (and their interaction in the most complex model), the best model fit is achieved by the simplest model with only patient as random effect ($\Delta BIC >= 23.6$).

Broadband cluster permutation tests

Non-parametric cluster permutation tests were carried out in the frequency ranges 1-90 Hz, and 160-390 Hz. Time-frequency cells post-stimulation were compared to the average power per frequency in the baseline period for each patient. As the time-frequency matrices for the conditions had to be matched in size and for computational convenience the time axes were matched to the shortest cleaned baseline segment of 44 s. Several data sets were excluded from cluster analyses due to strong variability between trials and broadband spectral artifacts depending on the frequency bands included in the analysis. The permutation tests yielded no significant clusters at the alpha = 0.05 level for neither of the stimulation conditions (see Figure 7).

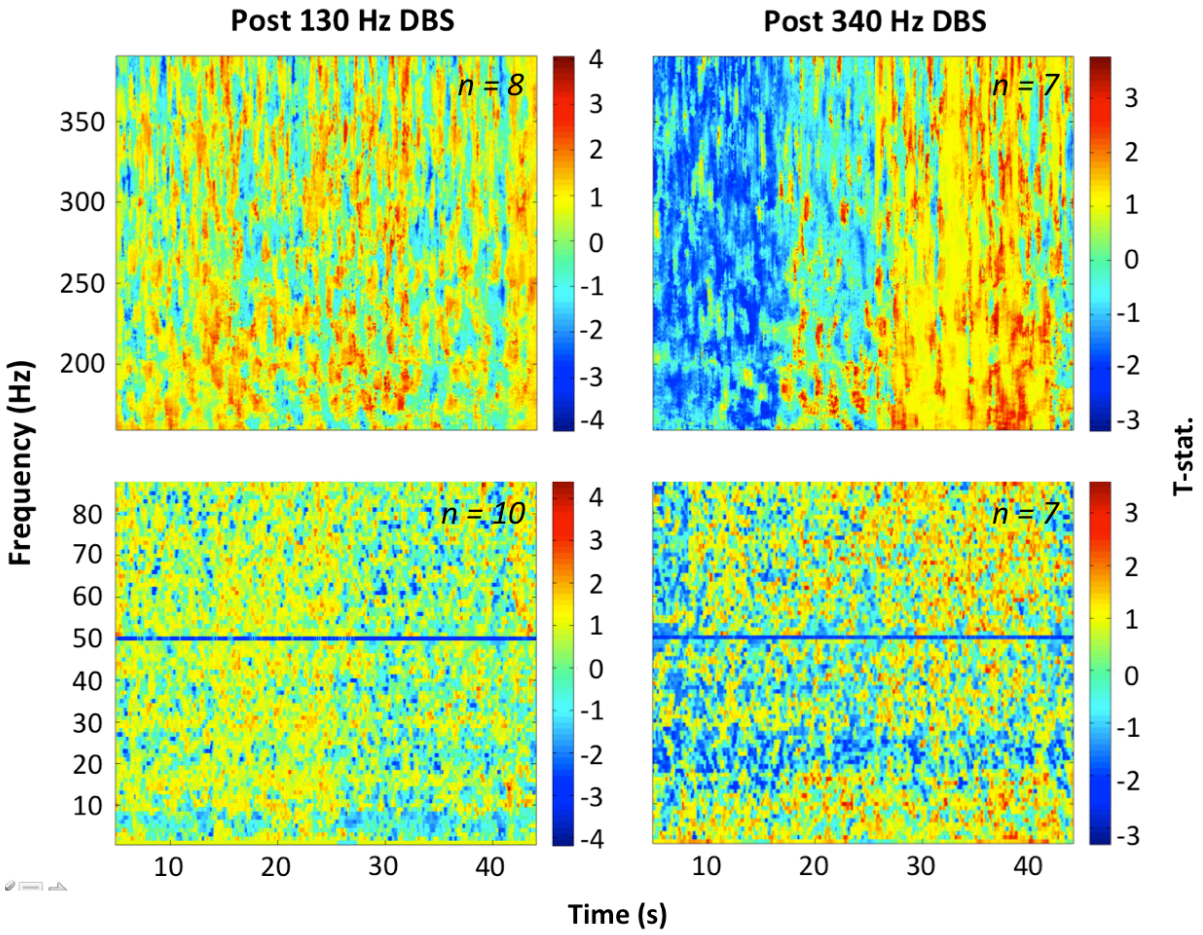

Figure 7. Output of the post-DBS cluster permutation tests per stimulation frequency for both low and high frequency oscillations (1-90 Hz, and 160-390 Hz, respectively). The z-axis denotes t-values used to calculate the cluster-sum t-statistics. Outside of the notch-filtered 50 Hz frequency band there are no significant clusters.

Discussion

Our goal was to investigate the oscillatory effects of subthalamic DBS at different frequencies (130 Hz and 340 Hz) on the contralateral STN during stimulation and both STN after DBS. First, we predicted reduced β-band activity as a result of DBS for both hemispheres, which was expected to slowly normalize after DBS OFF. Secondly, a similar effect for slow wave oscillations below 7 Hz was expected. Thirdly, HFOs were hypothesized to fluctuate roughly around the 250 Hz and 350 Hz bands as a result of DBS in such a way that the power ratio between these two bands shifts in favor of the 350 Hz band due to

stimulation. Finally, both stimulation frequencies were expected to lead to the aforementioned effects and differences between those conditions were predicted to most likely occur for HFOs.

To our knowledge the effects of DBS on the neuronal dynamics of the contralateral STN have not previously been investigated. Unfortunately, due to prominent artifacts during active stimulation, analyses were limited to the post-stimulation period and contralateral channels. This study nevertheless provides important insights into both the study of contralateral STN activity relative to the DBS locus, as well as LFP recordings from the Parkinsonian STN in general. First of all, the finding of strong artifactual activity measured from the contralateral hemisphere relative to the artifact's source is useful in itself. Secondly, the absence of significant oscillatory effects in the post-DBS period, and especially the absence of obvious β-peaks at rest for many patients are indicative of a more complex oscillatory profile across patients than sometimes hypothesized.

High variability in resting state β-peak signatures

The absence of a significant difference between post-stimulation and baseline β-peak-power is logical, as many of the selected channels did not show a prominent β-peak in the baseline period (see Figure 4). That absence, however, is surprising given that previous studies have shown that in an unmedicated resting state the vast majority of Parkinsonian STN display prominent β-synchrony (Wingeier et al., 2006; Kühn et al., 2008; Ray et al., 2008; Bronte-Stewart et al., 2009; Kühn et al., 2009). How can these findings be reconciled?

Spatial differences. Potentially, lack of synchronized resting state β-profiles could be explained by not selecting the correct channels, possibly recording activity outside the STN or in the wrong STN region, as increased β-power is associated with the dorsal part of the STN (Chen et al., 2006), similar to coupling of HFO amplitude to β-phase and β-spike-phase locking (Yang et al., 2014). However, selecting the channel with the highest absolute β-power

is the same technique used by the groups who previously analyzed DBS effects on STN β-activity (Wingeier et al., 2006; Kühn et al., 2008, Bronte-Stewart et al., 2009). This method has furthermore been shown to signify good support for STN localization during intra-surgical recordings (Chen et al., 2006), as well as post-operatively via neuroimaging (Kühn et al., 2008). Importantly, visual inspection of all bipolar montages of adjacent contacts does not reveal obvious peaks in the β-band for unselected channels even for more liberal β-ranges rendering a mismatch in spatial selection between studies implausible for explaining the discrepant findings (see Figure S1, note that p2 and p4 were deleted from all analyses).

Definitions of β-profiles. The method for calculating peak-power was less focused on narrow peaks compared to prior work (e.g. Kühn et al., 2008) and encompassed a wider frequency range. Yet, this only steers our statistical analyses towards finding broader changes in β-synchrony, possibly losing some statistical power if the β-peak effect is narrower. It does not explain the absence of spectral peaks at baseline, which in any case seem to be quite variable in bandwidth between patients (e.g. Bronte-Stewart et al., 2009). Another source of variability between studies lies in the frequency ranges considered as β-band, with Kühn et al. (2008) taking the 13 - 30 Hz band, Bronte-Stewart and colleagues using 13 - 35 Hz power, and Wingeier et al. (2006) selecting an individual β-band in the 10 - 40 Hz range depending on a conjoint spectral peak in at least two adjacent bipolar channel pairs per STN at rest and a relative decrease during movement. Nevertheless, these differences mostly suggest that several definitions of β-band power yield sensible channel selections. Again, visual inspection of periodograms does not suggest that we missed peaks due to our defined frequency range (Figure S1).

Patient differences. Individual differences between PD patients who undergo DBS are quite large (see Table 1), and it seems reasonable that factors such as age, disease duration, as well as symptom composition might be related to the extent that subthalamic DBS affects oscillatory neural dynamics. For example, the hypothesized pathological

β-synchrony has been associated with bradykinesia and rigidity, but not tremor (see Beuter et al., 2014). Nevertheless, as patients selected for DBS surgery are in the advanced stages of the disease bradykinesia and rigidity symptoms are quite prevalent throughout the sample, irrespective of tremor scores (note that Table 1 shows UPDRS scores without tremor).

Ultimately, it is unclear why the techniques previously used for channel selection to record STN activity show such discrepant spectral patterns in this patient sample. The data suggests that increased synchrony in the β-band of resting state STN activity of PD patients who underwent surgery might not be as common as previously thought. Interestingly, one of the cleanest data sets did show prominent β-suppression that slowly normalized in the post-DBS period relative to baseline (see Figure S3, p10).

Caveats and suggested improvements

Time-frequency data. The vacancy of significant clusters in any of the other analyzed frequency bands (1-90 Hz, 160-390 Hz) comparing baseline to post-DBS is not particularly informative, given the large variation in power between post-stimulation periods within patients. This also applies to β-peak power, but to a lesser extent as often artifacts emerged over higher broadband spectral windows. However, this was still a problem for the cluster permutation, because we opted for a wide spectral range including higher frequencies. Cluster permutation tests are also biased against finding short-lived effects as we included 44 s post-stimulation. We decided to exclude some of the patients' data sets completely from the cluster analysis in order to somewhat improve the signal to noise ratio. Which data sets to exclude was based on visual inspection of time-frequency representations averaged over trials for each patient. However, the resulting sample sizes for calculation of the cluster permutation test were too small to have a high likelihood of finding real effects. Moreover, given the sparse number of trials per patient variation within patients was still considerable. Finally, the grid of time-frequency cells might have been too finely woven. For example, smoothing the

data in the time domain would have facilitated the construction of significant clusters, as variability between successive cells would have been reduced. Alternatively and additionally, a different cluster statistic might have been employed. For example, a cluster-averaged t-statistic does not value large clusters over smaller ones. That way a short-lived narrow band effect would not be obscured by a more broadband or long-lived effect, as is the case for cluster-summed t-statistics.

Artifact rejection. A potential solution to the lack of data is to refrain from omitting muscle and tremor artifacts defined via EMG electrode inspection from LFP analyses. This was tried for some data sets to get a qualitative impression and lead to more time points being retained. Despite this data quality was still poor. Nevertheless, using such an approach would have been preferable. Another potential issue in this study was that visually inspecting data in the time-domain after deleting EMG muscle artifacts might not be sufficient to thoroughly clean the data. It was considered to also survey single trial time-frequency data for artifact rejection. However, given the already low number of trials and missing data within trials, as well as time constraints we decided against it.

Future directions

One important follow up analysis on these results is to create spatial maps of the electrode leads from post-operative MRI images in order to verify placement within the STN. An interesting next step would be to look at MEG scalp recordings, effects of DBS on cortical activity, as well as subcortico-cortical interactions. Other fascinating points of inquiry are in what way subcortical regions are coupled with each other, and in what way STN HFO amplitude locks to β-phase. Admittedly, it seems plausible that missing β-peaks at baseline allude to an absence of β-HFO PAC as well. Nevertheless, such a finding would give some added understanding of subcortical oscillatory dynamics in PD, being in line with the hypothesis that increased β-power exerts negative effects on motor processing through an

entrapment of HFO amplitude (for a discussion see Storzer et al., 2015). Finally, the oscillatory subcortical and cortical dynamics associated with tremor episodes should be explored (see Hirschmann et al., 2013). For example, α-band synchrony has been shown to correlate with tremor activity (see Beuter et al., 2014). Regrettably, these analyses were beyond the scope of this master thesis.

Conclusion

Electrical stimulation of the STN is an effective treatment for PD symptoms, yet its mechanism of action remains unknown. Oscillatory neural signals are a promising source for understanding the connection between brain activity, symptoms and treatment. A difficulty lies in discerning physiological activity from stimulation related artifacts. In this study, we aimed to elucidate neuronal dynamics in response to DBS by probing the STN of the contralateral hemisphere relative to stimulation. Albeit not being able to discern subcortical activity from artifacts during DBS, as well as not observing oscillatory changes on the group level after ceasing DBS, we can still draw some qualitative conclusions about oscillatory effects in the Parkinsonian STN: 1) The stimulation artifact can obscure physiological brain activity recorded at the contralateral STN; 2) visual inspection indicates that there might be DBS after-effects in terms of β-suppression for some, but not all STN, probably depending on the degree of increased synchrony prior to DBS, and 3) individualized β-peaks do not seem to be as prevalent in the Parkinsonian STN as previously thought.

References

Albin, R. L., Young, A. B., Penney, J. B., Roger, L. A., & Young, B. B. (1989). The functional anatomy of basal ganglia disorders. *Perspectives on Disease*, *12*(10), 366–375.

Baguley, T. (2012). Calculating and graphing within-subject confidence intervals for ANOVA. *Behavior research methods*, 158–175. doi:10.3758/s13428-011-0123-7

Bates, D., Maechler, M., & Bolker, B. (2011). lme4: Linear mixed-effects models using S4 classes (Version 0.999999-2) [computer software]. Available from http://CRAN.R-project.org/package=lme4

Beaulieu, J., & Gainetdinov, R. R. (2011). The Physiology , Signaling , and Pharmacology of Dopamine Receptors, *63*(1), 182–217. doi:10.1124/pr.110.002642.182

Belluscio, M. A., Escande, M. V., Keifman, E., Riquelme, L. A., Murer, M. G., & Zold, C. L. (2014). Oscillations in the basal ganglia in Parkinson's disease: Role of the striatum. *Basal Ganglia*, *3*(4), 203–212. doi:10.1016/j.baga.2013.11.003

Bergman, H., Feingold, a, Nini, a, Raz, a, Slovin, H., Abeles, M., & Vaadia, E. (1998). Physiological aspects of information processing in the basal ganglia of normal and parkinsonian primates. *Trends in Neurosciences*, *21*(1), 32–8. Retrieved from http://www.ncbi.nlm.nih.gov/pubmed/9464684

Beuter, A., Lefaucheur, J.-P., & Modolo, J. (2014). Closed-loop cortical neuromodulation in Parkinson's disease: An alternative to deep brain stimulation? *Clinical Neurophysiology : Official Journal of the International Federation of Clinical Neurophysiology*, *125*(5), 874–885. doi:10.1016/j.clinph.2014.01.006

Brittain, J.-S., & Brown, P. (2014). Oscillations and the basal ganglia: Motor control and beyond. *NeuroImage*, *85*, 637–647. doi:10.1016/j.neuroimage.2013.05.084

Bronte-Stewart, H., Barberini, C., Koop, M. M., Hill, B. C., Henderson, J. M., & Wingeier, B. (2009). The STN β-band profile in Parkinson's disease is stationary and shows

prolonged attenuation after deep brain stimulation. *Experimental Neurology*, *215*(1), 20–8. doi:10.1016/j.expneurol.2008.09.008

Buzsáki, G., & Draguhn, A. (2004). Neuronal oscillations in cortical networks. *Science (New York, N.Y.)*, *304*(5679), 1926–9. doi:10.1126/science.1099745

Chen, C. C., Lin, W. Y., Chan, H. L., Hsu, Y. T., Tu, P. H., Lee, S. T., … Brown, P. (2011). Stimulation of the subthalamic region at 20 Hz slows the development of grip force in Parkinson's disease. *Experimental Neurology*, *231*(1), 91–6. doi:10.1016/j.expneurol.2011.05.018

Chen, C. C., Pogosyan, A., Zrinzo, L. U., Tisch, S., Limousin, P., Ashkan, K., … Brown, P. (2006). Intra-operative recordings of local field potentials can help localize the subthalamic nucleus in Parkinson's disease surgery. *Experimental Neurology*, *198*(1), 214–21. doi:10.1016/j.expneurol.2005.11.019

Chinta, S. J., & Andersen, J. K. (2005). Dopaminergic neurons. *The International Journal of Biochemistry & Cell Biology*, *37*(5), 942–6. doi:10.1016/j.biocel.2004.09.009

Cousineau, D. (2005). Confidence intervals in within-subject designs : A simpler solution to Loftus and Masson's method, *1*(1), 42–45.

Darvas, F., & Hebb, A. O. (2014). Task specific inter-hemispheric coupling in human subthalamic nuclei. *Frontiers in Human Neuroscience*, *8*(September), 701. doi:10.3389/fnhum.2014.00701

Eusebio, A., Chen, C. C., Lu, C. S., Lee, S. T., Tsai, C. H., Limousin, P., … Brown, P. (2008). Effects of low-frequency stimulation of the subthalamic nucleus on movement in Parkinson's disease. *Experimental Neurology*, *209*(1), 125–30. doi:10.1016/j.expneurol.2007.09.007

Eusebio, A., & Brown, P. (2009). Synchronisation in the β frequency-band--the bad boy of parkinsonism or an innocent bystander? *Experimental Neurology*, *217*(1), 1–3. doi:10.1016/j.expneurol.2009.02.003

Eusebio, a, Thevathasan, W., Doyle Gaynor, L., Pogosyan, a, Bye, E., Foltynie, T., Zrinzo, L., Ashkan, K., Aziz, T., & Brown, P. (2011). Deep brain stimulation can suppress pathological synchronisation in parkinsonian patients. *Journal of Neurology, Neurosurgery, and Psychiatry*, *82*(5), 569–73. doi:10.1136/jnnp.2010.217489

Eusebio, A., Cagnan, H., & Brown, P. (2012). Does suppression of oscillatory synchronisation mediate some of the therapeutic effects of DBS in patients with Parkinson's disease? *Frontiers in Integrative Neuroscience*, *6*(July), 47. doi:10.3389/fnint.2012.00047

Fasano, A., Daniele, A., & Albanese, A. (2012). Treatment of motor and non-motor features of Parkinson's disease with deep brain stimulation. Lancet Neurology, 11(5), 429–42. doi:10.1016/S1474-4422(12)70049-2

Foffani, G., Ardolino, G., Egidi, M., Caputo, E., Bossi, B., & Priori, a. (2006). Subthalamic oscillatory activities at β or higher frequency do not change after high-frequency DBS in Parkinson's disease. *Brain Research Bulletin*, *69*(2), 123–30. doi:10.1016/j.brainresbull.2005.11.012

Garcia, L., D'Alessandro, G., Bioulac, B., & Hammond, C. (2005). High-frequency stimulation in Parkinson's disease: more or less? *Trends in Neurosciences*, *28*(4), 209–16. doi:10.1016/j.tins.2005.02.005

Giannicola, G., Marceglia, S., Rossi, L., Mrakic-Sposta, S., Rampini, P., Tamma, F., … Priori, A. (2010). The effects of levodopa and ongoing deep brain stimulation on subthalamic β oscillations in Parkinson's disease. *Experimental Neurology*, *226*(1), 120–7. doi:10.1016/j.expneurol.2010.08.011

Hammond, C., Bergman, H., & Brown, P. (2007). Pathological synchronization in Parkinson's disease: networks, models and treatments. *Trends in Neurosciences*, *30*(7), 357–64. doi:10.1016/j.tins.2007.05.004

Hirschmann, J., Özkurt, T. E., Butz, M., Homburger, M., Elben, S., Hartmann, C. J., … Schnitzler, a. (2011). Distinct oscillatory STN-cortical loops revealed by simultaneous MEG and local field potential recordings in patients with Parkinson's disease. *NeuroImage*, *55*(3), 1159–68. doi:10.1016/j.neuroimage.2010.11.063

Hirschmann, J., Hartmann, C. J., Butz, M., Hoogenboom, N., Ozkurt, T. E., Elben, S., … Schnitzler, A. (2013). A direct relationship between oscillatory subthalamic nucleus-cortex coupling and rest tremor in Parkinson's disease. *Brain : A Journal of Neurology*. doi:10.1093/brain/awt271

Hung, H.-Y., Tsai, S.-T., Lin, S.-H., Jiang, J.-L., & Chen, S.-Y. (2013). Uneven benefits of subthalamic nucleus deep brain stimulation in Parkinson's disease - A 7-year cross-sectional study. *Tzu Chi Medical Journal*, *25*(4), 239–245. doi:10.1016/j.tcmj.2013.08.003

Darvas, F., & Hebb, A. O. (2014). Task specific inter-hemispheric coupling in human subthalamic nuclei. *Frontiers in Human Neuroscience*, *8*(September), 701. doi:10.3389/fnhum.2014.00701

Jankovic, J. (2008). Parkinson's disease: clinical features and diagnosis. *Journal of Neurology, Neurosurgery, and Psychiatry*, *79*(4), 368–76. doi:10.1136/jnnp.2007.131045

Jenkinson, N., Kühn, A. a, & Brown, P. (2013). Γ Oscillations in the Human Basal Ganglia. *Experimental Neurology*, *245*, 72–6. doi:10.1016/j.expneurol.2012.07.005

Joundi, R. a, Jenkinson, N., Brittain, J.-S., Aziz, T. Z., & Brown, P. (2012a). Driving oscillatory activity in the human cortex enhances motor performance. *Current Biology : CB*, *22*(5), 403–7. doi:10.1016/j.cub.2012.01.024

Joundi, R. a, Brittain, J.-S., Green, A. L., Aziz, T. Z., Brown, P., & Jenkinson, N. (2012b). Oscillatory activity in the subthalamic nucleus during arm reaching in Parkinson's disease. *Experimental Neurology*, *236*(2), 319–26. doi:10.1016/j.expneurol.2012.05.013

Kocabicak, E., Tan, S. K. H., & Temel, Y. (2012). Deep brain stimulation of the subthalamic nucleus in Parkinson's disease: Why so successful? *Surgical Neurology International*, *3*(Suppl 4), S312–4. doi:10.4103/2152-7806.103024

Kravitz, A. V, Freeze, B. S., Parker, P. R. L., Kay, K., Myo, T., Deisseroth, K., & Kreitzer, A. C. (2010). Regulation of parkinsonian motor behaviors by optogenetic control of basal ganglia circuitry. *Nature*, *466*(7306), 622–626. doi:10.1038/nature09159.Regulation

Kühn, A. a, Kupsch, A., Schneider, G.-H., & Brown, P. (2006). Reduction in subthalamic 8-35 Hz oscillatory activity correlates with clinical improvement in Parkinson's disease. *The European Journal of Neuroscience*, *23*(7), 1956–60. doi:10.1111/j.1460-9568.2006.04717.x

Kühn, A. a, Kempf, F., Brücke, C., Gaynor Doyle, L., Martinez-Torres, I., Pogosyan, A., … Brown, P. (2008). High-frequency stimulation of the subthalamic nucleus suppresses oscillatory β activity in patients with Parkinson's disease in parallel with improvement in motor performance. *The Journal of Neuroscience : The Official Journal of the Society for Neuroscience*, *28*(24), 6165–73. doi:10.1523/JNEUROSCI.0282-08.2008

Kühn, A. a, Tsui, A., Aziz, T., Ray, N., Brücke, C., Kupsch, A., … Brown, P. (2009). Pathological synchronisation in the subthalamic nucleus of patients with Parkinson's disease relates to both bradykinesia and rigidity. *Experimental Neurology*, *215*(2), 380–7. doi:10.1016/j.expneurol.2008.11.008

Lanciego, J. L., Luquin, N., & Obeso, J. a. (2012). Functional neuroanatomy of the basal ganglia. *Cold Spring Harbor Perspectives in Medicine*, *2*(12), a009621. doi:10.1101/cshperspect.a009621

Lawrence, M. A. (2012). ez: Easy analysis and visualization of factorial experiments (Version 4.1-1) [computer software]. Available from http://CRAN.R-project.org/package=ez

Litvak, V., Jha, A., Eusebio, A., Oostenveld, R., Foltynie, T., Limousin, … Brown, P. (2011). Resting oscillatory cortico-subthalamic connectivity in patients with Parkinson's disease. *Brain : A Journal of Neurology*, *134*(Pt 2), 359–74. doi:10.1093/brain/awq332

Little, S., Pogosyan, A., Kuhn, A. A., & Brown, P. (2012). β band stability over time correlates with Parkinsonian rigidity and bradykinesia. *Experimental Neurology*, *236*(2), 383–8. doi:10.1016/j.expneurol.2012.04.024

López-Azcárate, J., Tainta, M., Rodríguez-Oroz, M. C., Valencia, M., González, R., Guridi, J., … Alegre, M. (2010). Coupling between β and high-frequency activity in the human subthalamic nucleus may be a pathophysiological mechanism in Parkinson's disease. *The Journal of Neuroscience : The Official Journal of the Society for Neuroscience*, *30*(19), 6667–77. doi:10.1523/JNEUROSCI.5459-09.2010

Mallet, N., Pogosyan, A., Sharott, A., Csicsvari, J., Bolam, J. P., Brown, P., & Magill, P. J. (2008). Disrupted dopamine transmission and the emergence of exaggerated β oscillations in subthalamic nucleus and cerebral cortex. *The Journal of Neuroscience : The Official Journal of the Society for Neuroscience*, *28*(18), 4795–806. doi:10.1523/JNEUROSCI.0123-08.2008

Maranis, S., Tsouli, S., & Konitsiotis, S. (2011). Treatment of motor symptoms in advanced Parkinson's disease: a practical approach. *Progress in Neuro-Psychopharmacology & Biological Psychiatry*, *35*(8), 1795–807. doi:10.1016/j.pnpbp.2011.05.014

Maris, E., & Oostenveld, R. (2007). Nonparametric statistical testing of EEG- and MEG-data. *Journal of Neuroscience Methods*, *164*(1), 177–90. doi:10.1016/j.jneumeth.2007.03.024

McIntyre, C. C., & Hahn, P. J. (2010). Network perspectives on the mechanisms of deep brain stimulation. *Neurobiology of Disease*, *38*(3), 329–37. doi:10.1016/j.nbd.2009.09.022

Morey, R. D. (2008). Confidence Intervals from Normalized Data: A correction to Cousineau (2005). *Tutorial in Quantitative Methods for Psychology*, *4*(2), 61–64.

Nambu, A. (2008). Seven problems on the basal ganglia. *Current Opinion in Neurobiology*, *18*(6), 595–604. doi:10.1016/j.conb.2008.11.001

Ohtsuka, C., Sasaki, M., Konno, K., Koide, M., Kato, K., Takahashi, J., … Terayama, Y. (2013). Changes in substantia nigra and locus coeruleus in patients with early-stage Parkinson's disease using neuromelanin-sensitive MR imaging. *Neuroscience letters*, *541*, 93–8. doi:10.1016/j.neulet.2013.02.012

Olanow, C. W., & Brundin, P. (2013). Parkinson's disease and alpha synuclein: is Parkinson's disease a prion-like disorder? *Movement Disorders : Official Journal of the Movement Disorder Society*, *28*(1), 31–40. doi:10.1002/mds.25373

Olejnik, S., & Algina, J. (2003). Generalized eta and omega squared statistics: Measures of effect size for some common research designs. *Psychological Methods*, *8*, 434-447.

Oostenveld, R., Fries, P., Maris, E., & Schoffelen, J.M. (2011). FieldTrip: Open Source Software for Advanced Analysis of MEG, EEG, and Invasive Electrophysiological Data. *Computational Intelligence and Neuroscience, 9,* Article ID 156869, doi:10.1155/2011/156869

Oswal, A., Brown, P., & Litvak, V. (2013a). Movement related dynamics of subthalmo-cortical alpha connectivity in Parkinson's disease. *NeuroImage*, *70*, 132–42. doi:10.1016/j.neuroimage.2012.12.041

Oswal, A., Brown, P., & Litvak, V. (2013b). Synchronized neural oscillations and the pathophysiology of Parkinson's disease. *Current Opinion in Neurology*, *26*(6), 662–70. doi:10.1097/WCO.0000000000000034

Özkurt, T. E., Butz, M., Homburger, M., Elben, S., Vesper, J., Wojtecki, L., & Schnitzler, A. (2011). High frequency oscillations in the subthalamic nucleus: a neurophysiological marker of the motor state in Parkinson's disease. *Experimental Neurology*, *229*(2), 324–31. doi:10.1016/j.expneurol.2011.02.015

Priori, a, Ardolino, G., Marceglia, S., Mrakic-Sposta, S., Locatelli, M., Tamma, F., … Foffani, G. (2006). Low-frequency subthalamic oscillations increase after deep brain stimulation in Parkinson's disease. *Brain Research Bulletin*, *71*(1-3), 149–54. doi:10.1016/j.brainresbull.2006.08.015

Puschmann, A. (2013). Monogenic Parkinson's disease and parkinsonism: clinical phenotypes and frequencies of known mutations. *Parkinsonism & Related Disorders*, *19*(4), 407–15. doi:10.1016/j.parkreldis.2013.01.020

R Core Team (2012). R: A language and environment for statistical computing. R Foundation for Statistical Computing, Vienna, Austria. ISBN 3-900051-07-0, URL http://www.R-project.org/.

Ray, N. J., Jenkinson, N., Wang, S., Holland, P., Brittain, J. S., Joint, C., … Aziz, T. (2008). Local field potential β activity in the subthalamic nucleus of patients with Parkinson's disease is associated with improvements in bradykinesia after dopamine and deep brain stimulation. *Experimental Neurology*, *213*(1), 108–13. doi:10.1016/j.expneurol.2008.05.008

Rossi, L., Marceglia, S., Foffani, G., Cogiamanian, F., Tamma, F., Rampini, P., … Priori, a. (2008). Subthalamic local field potential oscillations during ongoing deep brain stimulation in Parkinson's disease. *Brain Research Bulletin*, *76*(5), 512–21. doi:10.1016/j.brainresbull.2008.01.023

Shemisa, K., Hass, C. J., Foote, K. D., Okun, M. S., Wu, S. S., Jacobson, C. E., … Fernandez, H. H. (2011). Unilateral deep brain stimulation surgery in Parkinson's disease improves ipsilateral symptoms regardless of laterality. *Parkinsonism & Related Disorders*, *17*(10), 745–8. doi:10.1016/j.parkreldis.2011.07.010

Silberstein, P., Kühn, A. a, Kupsch, A., Trottenberg, T., Krauss, J. K., Wöhrle, J. C., … Brown, P. (2003). Patterning of globus pallidus local field potentials differs between

Parkinson's disease and dystonia. *Brain : A Journal of Neurology*, *126*(Pt 12), 2597–608. doi:10.1093/brain/awg267

Storzer, L., Burgers, S., & Hirschmann, J. (2015). Are Beta Phase-Coupled High-Frequency Oscillations and Beta Phase-Locked Spiking Two Sides of the Same Coin? *Journal of Neuroscience*, *35*(5), 1819–1820. doi:10.1523/JNEUROSCI.4647-14.2015

Sung, V. W., & Nicholas, A. P. (2013). Nonmotor symptoms in Parkinson's disease: expanding the view of Parkinson's disease beyond a pure motor, pure dopaminergic problem. *Neurologic Clinics*, *31*(3 Suppl), S1–16. doi:10.1016/j.ncl.2013.04.013

Tan, L. C. S., (2013). Epidemiology of Parkinson disease. *Neurology Asia*, *18*(3), 231–238.

The Mathworks Inc. (2010). MATLAB the language of technical computing (Version 8.3.0.532 (R2014a)) [computer software]. Natick: Massachusetts, United States. Available from http://www.mathworks.nl/products/matlab/

Thomson, D. (1982). Spectrum estimation and harmonic analysis. *Proc. IEEE 70*, 1055–1096

Tsang, E. W., Hamani, C., Moro, E., Mazzella, F., Saha, U., Lozano, … Chen, R. (2012). Subthalamic deep brain stimulation at individualized frequencies for Parkinson disease. *Neurology*, *78*(24), 1930–8. doi:10.1212/WNL.0b013e318259e183

Tseng, K. Y., Kasanetz, F., Kargieman, L., Riquelme, L. a, & Murer, M. G. (2001). Cortical slow oscillatory activity is reflected in the membrane potential and spike trains of striatal neurons in rats with chronic nigrostriatal lesions. *The Journal of Neuroscience : The Official Journal of the Society for Neuroscience*, *21*(16), 6430–9. Retrieved from http://www.ncbi.nlm.nih.gov/pubmed/11487667

Welch, P. (1967). The use of fast Fourier transform for the estimation of power spectra: a method based on time averaging over short, modified periodograms. *IEEE Trans. Audio Electro. 15*, 70–73.

Wickham H. (2009). ggplot2: elegant graphics for data analysis. Springer New York.

Wingeier, B., Tcheng, T., Koop, M. M., Hill, B. C., Heit, G., & Bronte-Stewart, H. M. (2006). Intra-operative STN DBS attenuates the prominent β rhythm in the STN in Parkinson's disease. *Experimental Neurology*, *197*(1), 244–51. doi:10.1016/j.expneurol.2005.09.016

Xia, R., & Mao, Z.-H. (2012). Progression of motor symptoms in Parkinson's disease. *Neuroscience Bulletin*, *28*(1), 39–48. doi:10.1007/s12264-012-1050-z

Yang, a. I., Vanegas, N., Lungu, C., & Zaghloul, K. a. (2014). B-Coupled High-Frequency Activity and B-Locked Neuronal Spiking in the Subthalamic Nucleus of Parkinson's Disease. *Journal of Neuroscience*, *34*(38), 12816–12827. doi:10.1523/JNEUROSCI.1895-14.2014

Yoshida, F., Martinez-Torres, I., Pogosyan, A., Holl, E., Petersen, E., Chen, C. C., … Brown, P. (2010). Value of subthalamic nucleus local field potentials recordings in prediciting stimulation parameters for deep brain stimulation in Parkinson's disease. *J. Neurol. Neurosurg. Psychiatry* 81, 885–889.

Zold, C. L., Escande, M. V, Pomata, P. E., Riquelme, L. a, & Murer, M. G. (2012). Striatal NMDA receptors gate cortico-pallidal synchronization in a rat model of Parkinson's disease. *Neurobiology of Disease*, *47*(1), 38–48. doi:10.1016/j.nbd.2012.03.022

Appendix

Supplementary Figures

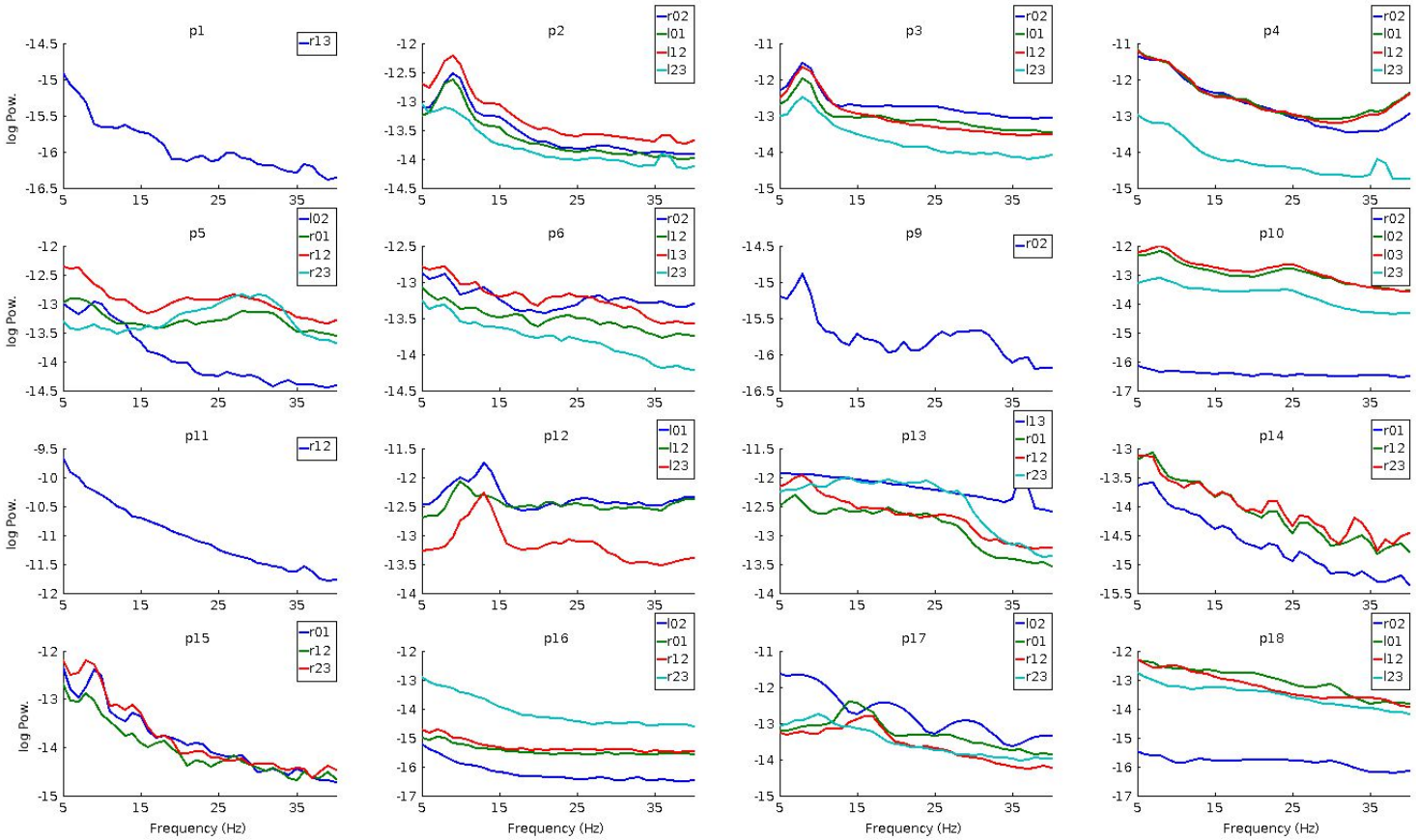

Figure S1. Power spectral density of all available adjacent bipolar channels on the contralateral side relative to DBS for a 30 s period of pre-stimulation baseline recordings.

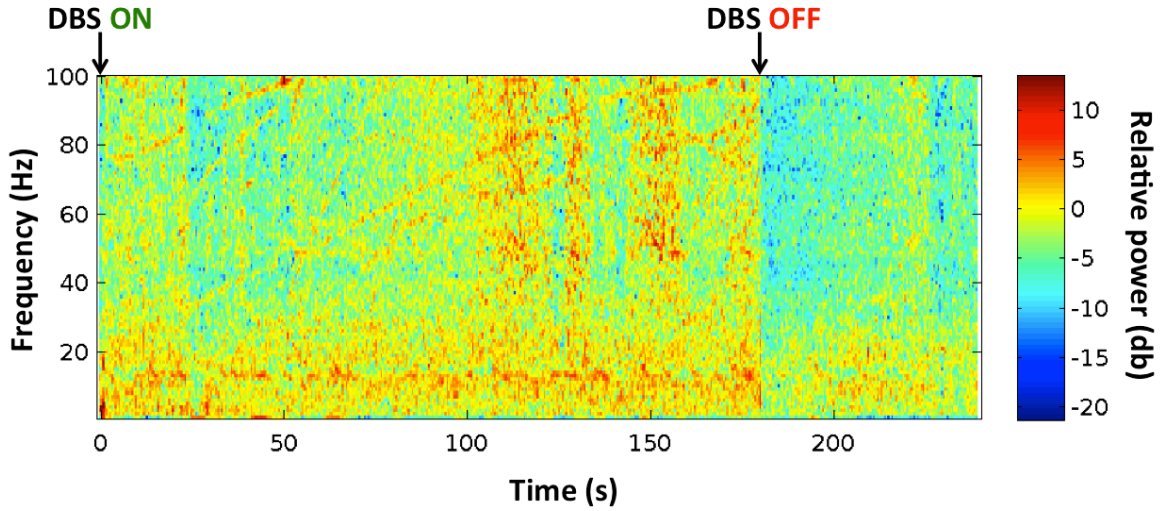

Figure S2. Spectrogram of 1 s data prior to DBS until 60 s after DBS averaged over trials for channel l01, contralateral to stimulation of patient p12. Note that some noise patterns disappear after stimulation OFF. Broadband power changes within stimulation and post-stimulation time periods are likely due to overall power differences between trials, but could also signify muscle activity. Z-axes denotes decibel scores relative to baseline (pre-DBS).

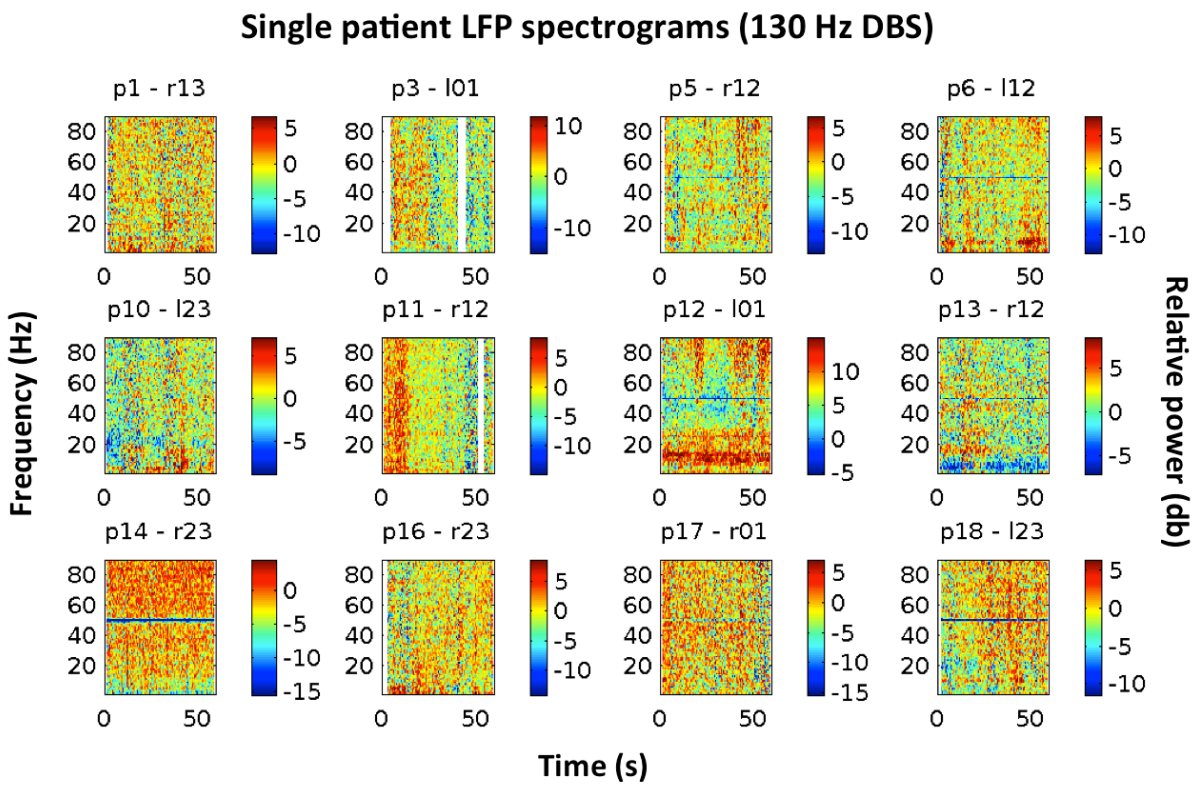

Figure S3. Spectrograms of the period post 130 Hz DBS averaged over trials for the contralateral channels relative to DBS. Color-coding denotes decibel changes in power relative to baseline (pre-DBS). Note the 20 Hz-centered suppression and slow normalization in the case of p10.

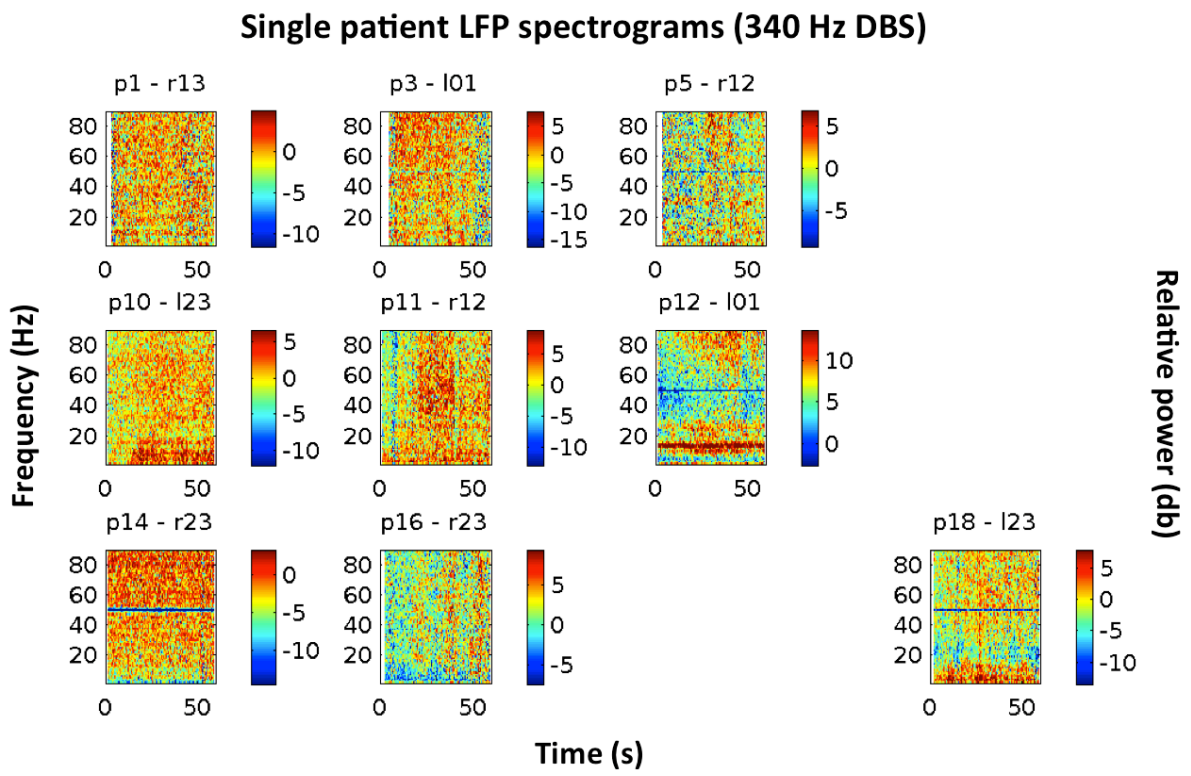

Figure S4. Spectrograms of post 340 Hz stimulation period averaged over trials. Decibel scores relative to baseline are displayed in color.